

LETTER TO THE EDITOR

An extended *Herschel* drop-out source in the center of AS1063: a 'normal' dusty galaxy at $z = 6.1$ or SZ substructures?

F. Boone^{1,2}, B. Clément³, J. Richard⁴, D. Schaerer^{5,2}, D. Lutz⁶, A. Weiß⁷, M. Zemcov⁸, E. Egami³, T. D. Rawle⁹, G. L. Walth³, J.-P. Kneib^{10,11}, F. Combes¹², I. Smail¹³, A. M. Swinbank¹³, B. Altieri⁹, A. W. Blain¹⁴, S. Chapman¹⁵, M. Dessauges-Zavadsky⁵, R. J. Ivison¹⁶, K. K. Knudsen¹⁷, A. Omont¹⁸, R. Pelló^{1,2}, P. G. Pérez-González¹⁹, I. Valtchanov⁹, P. van der Werf²⁰, and M. Zamojski⁵

¹ Université de Toulouse; UPS-OMP; IRAP; Toulouse, France

² CNRS; IRAP; 9 Av. colonel Roche, BP 44346, F-31028 Toulouse cedex 4, France

³ Steward Observatory, University of Arizona, 933 North Cherry Avenue, Tucson, AZ 85721, USA

⁴ Centre de Recherche Astrophysique de Lyon, Université Lyon 1, 9 Avenue Charles André, F-69561 Saint Genis Laval, France

⁵ Geneva Observatory, Université de Genève, 51 chemin des Maillettes, 1290 Versoix, Switzerland

⁶ Max-Planck-Institut für extraterrestrische Physik, Postfach 1312, 85741 Garching, Germany

⁷ Max-Planck-Institut für Radioastronomie, Auf dem Hügel 69, 53121 Bonn, Germany

⁸ Department of Physics, Mathematics, and Astronomy, California Institute of Technology, Pasadena, CA 91125, USA

⁹ European Space Astronomy Centre (ESAC)/ESA, Villanueva de la Cañada, E-28691 Madrid, Spain

¹⁰ Laboratoire d'astrophysique, Ecole Polytechnique Fédérale de Lausanne, Observatoire de Sauverny, 1290 Versoix, Switzerland

¹¹ Aix Marseille Université, CNRS, LAM, UMR 7326, 13388, Marseille, France

¹² LERMA, Observatoire de Paris, 61 avenue de l'Observatoire, 75014 Paris, France

¹³ Institute for Computational Cosmology, Department of Physics, Durham University, Durham DH1 3LE, UK

¹⁴ Physics & Astronomy, University of Leicester, Leicester, LE1 7RH, UK

¹⁵ Department of Physics and Atmospheric Science, Dalhousie University Halifax, NS, B3H 3J5, Canada

¹⁶ Institute for Astronomy, University of Edinburgh, Royal Observatory, Blackford Hill, Edinburgh EH9 3HJ, UK

¹⁷ Department of Earth and Space Science, Chalmers University of Technology, Onsala Space Observatory, 43992 Onsala, Sweden

¹⁸ UPMC Univ Paris 6, UMR 7095, Institut d'Astrophysique de Paris, 75014, Paris, France

¹⁹ Departamento de Astrofísica, Facultad de CC. Físicas, Universidad Complutense de Madrid, 28040 Madrid, Spain

²⁰ Leiden Observatory, Leiden University, P.O. box 9513, 2300 RA Leiden, The Netherlands

;

ABSTRACT

In the course of our $870\mu\text{m}$ APEX/LABOCA follow up of the *Herschel* Lensing Survey we have detected a source in AS1063 (RXJ2248.7-4431), that has no counterparts in any of the *Herschel* PACS/SPIRE bands, it is a *Herschel* 'drop-out' with $S_{870}/S_{500} \geq 0.5$. The $870\mu\text{m}$ emission is extended and centered on the brightest cluster galaxy suggesting either a multiply imaged background source or substructure in the Sunyaev-Zel'dovich (SZ) increment due to inhomogeneities in the hot cluster gas of this merging cluster. We discuss both interpretations with emphasis on the putative lensed source. Based on the observed properties and on our lens model we find that this source could be the first SMG with a moderate far infrared luminosity ($L_{\text{FIR}} < 10^{12}L_{\odot}$) detected so far at $z > 4$. In deep *HST* observations we identified a multiply imaged $z \sim 6$ source and we measured its spectroscopic redshift $z=6.107$ with VLT/FORS. This source could be associated with the putative SMG but it is most likely offset spatially by 10-30 kpc and they could be interacting galaxies. With a FIR luminosity in the range $[5 - 15] \times 10^{11}L_{\odot}$ corresponding to a star formation rate in the range $[80 - 260] M_{\odot} \text{yr}^{-1}$, this SMG would be more representative than the extreme starbursts usually detected at $z > 4$. With a total magnification of ~ 25 it would open a unique window to the 'normal' dusty galaxies at the end of the epoch of reionization.

Key words. galaxies:high-redshift, submillimeter: galaxies, galaxies: evolution

1. Introduction

Estimating the contribution of dust obscured star formation in the early Universe is essential to constrain the models of galaxy evolution and it has been a growing field of research since the late 1990s (e.g., Blain et al. 2002). Submillimeter (submm) surveys have proven to be very efficient at detecting distant dusty galaxies (also known as Submillimeter Galaxies, SMGs) owing to the negative K-correction and their redshift distribution was found to peak at $z \sim 2 - 3$ (Chapman et al. 2005).

With the advent of a new generation of submm instruments the hunt for the highest redshift SMGs progressed at a rapid pace

in recent years. The first SMG beyond $z = 5$ was discovered by Capak et al. (2011) with JCMT/AzTEC. Based on a *Herschel* detection and a 30m/EMIR follow up, Combes et al. (2012) discovered an interacting system of bright SMGs at $z = 5.243$. At the same time Walter et al. (2012) using IRAM instruments found that an SMG known for years in the Hubble deep field is actually a system of galaxies lying at $z = 5.2$. Following up on SPT bolometer observations Vieira et al. (2013), and Weiß et al. (2013) measured with ALMA the spectroscopic redshifts of 23 new SMGs out of which two are at $z > 5$. In parallel, Riechers et al. (2013) observed 'red' SMGs based on *Herschel* colors with CARMA and discovered the highest redshift SMG at $z = 6.34$.

Table 1. Photometry of the $870\mu\text{m}$ northern peak with the wavelengths (λ) in μm and the flux densities (S_ν) in mJy. The upper limits are at 3σ .

λ	24	70	100	160	250	350	500	870
S_ν	<0.06	<0.75	<1.2	<3.8	<7.2	<9.9	<12.3	7.6 ± 1.1

In terms of luminosity, however, all the SMGs detected so far beyond $z > 4$ are ultraluminous infrared galaxies¹ (ULIRGs) with $L_{\text{FIR}} > 10^{12} L_\odot$ or even hyperluminous infrared galaxies (HyLIRGs) with $L_{\text{FIR}} > 10^{13} L_\odot$, implying star formation rates $\gtrsim 10^3 M_\odot \text{yr}^{-1}$. As confirmed by recent ALMA number counts (Karim et al. 2013; Hatsukade et al. 2013) these extreme starbursts are not representative of the average population of dusty star forming galaxies at $z > 4$ and the luminous infrared galaxies (LIRGs) with $L_{\text{FIR}} \sim 10^{11} L_\odot$ that should represent the majority remain to be discovered. The lensing power provided by massive galaxy clusters is widely used to detect distant galaxies (e.g., Smail et al. 1997). However, the recent discovery of substructures in the Sunyaev-Zel’dovich (SZ) increment of interacting clusters (Korngut et al. 2011; Mroczkowski et al. 2012) may complicate the interpretation of submm observations. We report here the discovery of a good candidate for a normal star forming galaxy at $z = 6.1$ lensed by the cluster AS1063 (RXCJ2248.7-4431) and we discuss the possibility that this source could instead correspond to substructures in the SZ effect. We adopt the Λ CDM concordance cosmology: $H_0 = 71 \text{ km s}^{-1} \text{ Mpc}^{-1}$, $\Omega_M = 0.27$ and $\Omega_\Lambda = 0.73$.

2. Observations and data reduction

Herschel observations of AS1063 at 70, 100, 160, 250, 350 and $500\mu\text{m}$ were obtained as part of the *Herschel* Lensing Survey (program IDs: KPOT_eegami.1, OT2_trawle.3) as described by Egami et al. (2010) and Rawle et al. (2010). The full width at half maximum (FWHM) of the beams are $5.2''$, $7.7''$, $11.3''$, $18.1''$, 24.9 and $36.6''$, respectively.

Observations of AS1063 at $870\mu\text{m}$ with the Large APEX Bolometer Camera LABOCA (Siringo et al. 2009) were obtained in the frame of the LABOCA Lensing Survey, a large program coordinated between ESO and MPI (E187A0437A, M-087.F-0005-2011). The observations were carried out in April and May 2012 in excellent weather conditions with an average precipitable water vapor (PWV) of 0.5 mm. The spiral mapping pattern was chosen to cover a circular area of $\sim 8'$ in diameter centered on the clusters. Absolute flux calibration was achieved through observations of Mars, Uranus and Neptune as well as secondary calibrators and was found to be accurate within $\sim 10\%$ (rms). The atmospheric attenuation was determined via skydips every ~ 2 hours as well as from independent data from the APEX radiometer which measures the line of sight water vapor column every minute (see Siringo et al. 2009, for a more detailed description). Pointing was checked on the nearby quasars and found to be stable within $3''$ (rms). The data were reduced using the Bolometer array data Analysis software (BoA, Schuller et al. in prep.). The effective resolution of the maps is $24.3''$. The pixel noise RMS at the center of the map is $1.1 \text{ mJy beam}^{-1}$.

3. Results

The LABOCA map shows a source at the center of the cluster AS1063 (Fig. 1) that is extended at the resolution of LABOCA

¹ The lowest luminosity SMG detected so far at $z > 4$ has $L_{\text{FIR}} = 1.3 \times 10^{12} L_\odot$ and is at $z = 4.04$ (Knudsen et al. 2010)

(beam FWHM= $24.3''$) and centered on the brightest cluster galaxy (BCG). Its north-eastern part has no counterparts in any of the *Herschel* bands nor in the $24\mu\text{m}$ MIPS band; it is a very red *Herschel* drop-out. It peaks at $7.6\pm 1.1 \text{ mJy}$ and its $3\text{-}\sigma$ upper limit at $500\mu\text{m}$ is 13 mJy , implying a flux ratio $S_{870}/S_{500} \geq 0.5$.

Although the BCG is not detected with *Herschel* (Rawle et al. 2012), the south-western part of the $870\mu\text{m}$ source is partly blended with the emission coming from two lower redshift sources with spectroscopic redshifts $z = 0.6$ and 0.3 (Walth et al. in prep). To extract the source properties in this crowded field we applied a multiwavelength simultaneous fit of the maps assuming a modified black body SED shape (following Blain et al. 2003, with $\alpha = 2.9$ and $\beta = 1.5$) for all the sources. There are two free parameters per source corresponding to the FIR luminosity and the wavelength of the SED peak (determined by the dust temperature, T_d and the redshift z). In a first iteration we run the procedure with the two low- z sources only. The residuals are shown with green contours in the Fig. 2; they represent the $870\mu\text{m}$ foreground-deblended emission. The morphology and the distribution of this emission with respect to the critical lines, with two peaks on each side of the BCG—one to the northeast at 7.6 mJy and the other to the southwest at 5.3 mJy —suggest either a multiply imaged background source or substructures in the SZ increment. We discuss the two interpretations in turn in the following section.

4. Discussion

4.1. Photometry of a putative lensed source

In a second iteration we run the photometry procedure again to fit simultaneously two sources at the positions of the $870\mu\text{m}$ peaks in addition to the two low- z sources. We assume that the two $870\mu\text{m}$ sources are the images of a single lensed source, which implies a unique peak wavelength (same redshift and dust temperature) and a total of 7 free parameters. The χ^2 value gives us an indication of the quality of the fit, it is plotted against the redshift and the dust temperature of the lensed source in the Fig. 3 with contours indicating the confidence levels. At a given dust temperature, the $870\mu\text{m}$ flux and the *Herschel* upper limits impose a lower limit to the redshift. Thus, if we assume $T_d > 20 \text{ K}$ as observed in most SMGs including the lowest luminosities (see, e.g., Symeonidis et al. 2013; Magnelli et al. 2012, or Swinbank et al. submitted), then the source must be at $z \geq 2$. If $T_d = 30 \text{ K}$ (mean value for $L_{\text{FIR}} \sim 10^{11.5} L_\odot$ according to the same references), then the redshift must be ≥ 4 . In addition, if we assume $z < 7$, the observed (i.e., uncorrected for lensing) FIR luminosities of the two peaks must be $< 10^{13} L_\odot$ (Fig. 3).

4.2. Lens and source models

Based on the identification of 13 multiple image systems out of which 5 have a spectroscopic redshift and the others have a reliable photometric redshift, we have built a lens model of the cluster (Richard et al. in prep). The critical lines computed with this model for $z=6$ are shown in the Fig. 2 in red.

As shown on the left panel of Fig. 2, with this model we can reproduce the two $870\mu\text{m}$ peaks by assuming a single source modeled by a circular Gaussian of FWHM= 2 kpc at $z = 6$. Four images of the source, labeled L1, L2, L3 and L4, are actually formed in a classical quad configuration; their magnifications are 10.8, 3.7, 7.1 and 3.1, respectively for a total magnification $\mu=25.5$. The images L3 and L4 are $\sim 3\times$ fainter than L1 and are therefore at $\sim 2\sigma$, which is consistent with no detection. To ob-

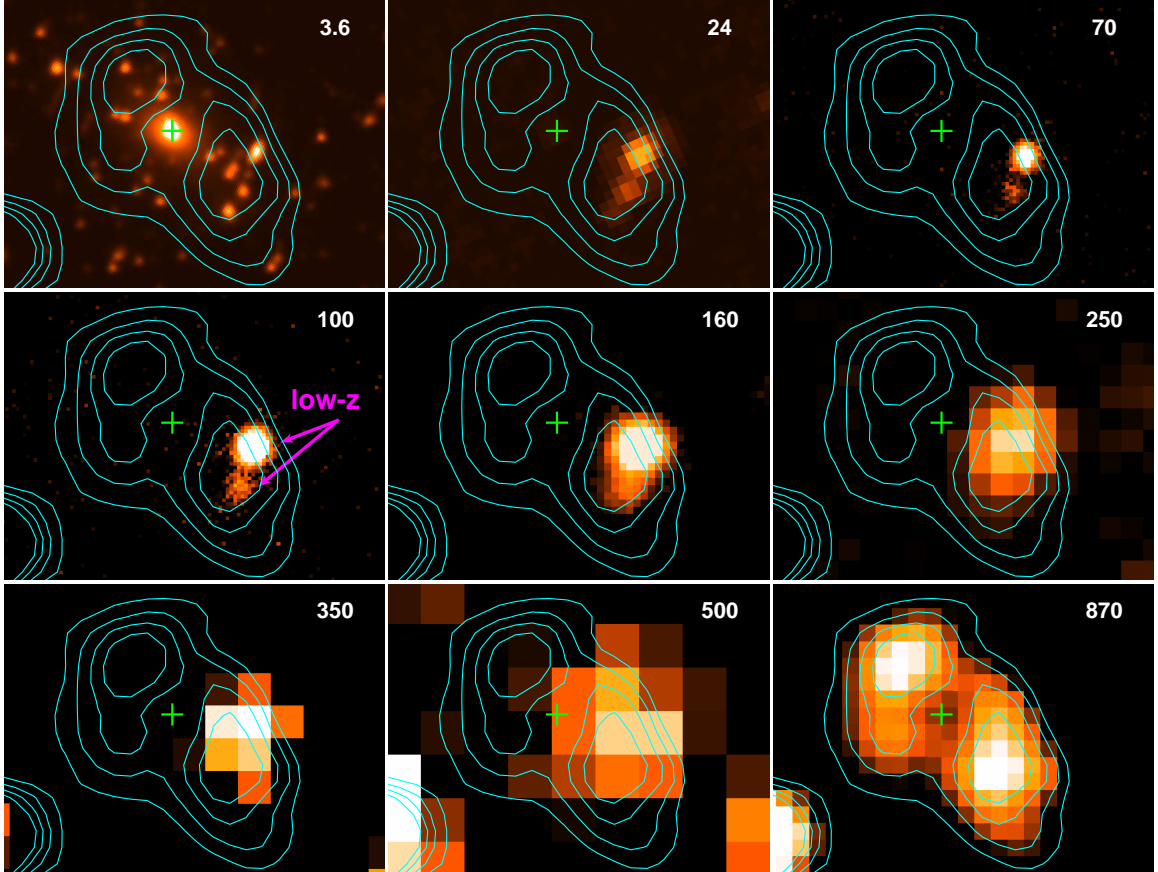


Fig. 1. $105'' \times 78''$ thumbnails showing the central region of the cluster AS1063 at 3.6, 24, 70, 100, 160, 250, 350, 500 and $870 \mu\text{m}$ (from left to right and from top to bottom). The contours correspond to the $870 \mu\text{m}$ emission detected with LABOCA at 3, 4, 5 and $6\text{-}\sigma$ ($\sigma = 1.1 \text{ mJy}$). The *Herschel* drop-out source can be seen around the BCG (marked by the green cross) at the center of the $870 \mu\text{m}$ map. The arrows in the $100 \mu\text{m}$ map point two low- z sources ($z = 0.3$ and 0.6), whose $870 \mu\text{m}$ emission is blended with the south-western part of the high- z source.

tain an L1-image brighter than the others it is required to align it with a galaxy of the cluster such that it undergoes an additional magnification. In this model the L1-image is formed close to two galaxies of the cluster. The differences between the model and the data are $\leq 3\sigma$. Because the angular distance between the two peaks (L1 and L2) decreases with decreasing redshift our lens model puts a strong constraint on the redshift, which must be ≥ 4 if we assume a single source. We note that it is possible that the southern source arises from lensing of a second background galaxy. However, this would imply multiple sources with similar very red SEDs.

Hence, according to our lens+source model and to the photometry, the luminosity of the putative lensed source corrected for lensing is likely $< 10^{12} L_{\odot}$, i.e., an order of magnitude lower than that of SMGs detected at $z > 4$ so far. For example, if we assume $T_d = 30 \text{ K}$ and $z = 6$, the observed luminosity of the northern peak is $L_{\text{FIR}} \sim 5 \times 10^{12} L_{\odot}$ (middle panel of Fig. 3), with $\mu_{\text{L1}} = 10$ this implies an intrinsic luminosity $L_{\text{FIR}} \sim 5 \times 10^{11} L_{\odot}$.

4.3. A plausible *HST* counterpart at $z = 6.107$

In the *HST* images and catalogs provided by the CLASH project we identified 4 objects (named 6.1, 6.2, 6.3 and 6.4 in Fig. 2 as in Richard et al. in prep), which could be the 4 images of a high- z source. Indeed, fitting various SED templates to the *HST* photometry we derived a redshift $z = 6.3 \pm 0.3$ (Fig 4) and the

image positions were accurately reproduced by our lens model for a source at $z \sim 6$. To confirm the redshift we recently obtained VLT/FORS spectroscopy of the 6.2, 6.3 and 6.4 images. The Ly- α line is clearly detected at $z = 6.107$ (Fig. 4)². The magnifications are $\mu_{6.1} = 17.1$, $\mu_{6.2} = 6.7$, $\mu_{6.3} = 5.9$ and $\mu_{6.4} = 2.5$.

The image 6.1 of this *HST* source benefits from a boost by the same two galaxies of the cluster as in the model discussed above for the $870 \mu\text{m}$ emission. However, if they are both at the same redshift the LABOCA source needs to be offset from the *HST* source to reproduce the southern peak (L2); it is at $\sim 30 \text{ kpc}$ in the above model. The distance between the two sources is mainly constrained by the flux ratio of the two $870 \mu\text{m}$ peaks, it could be in the range 10-30 kpc, suggesting interacting galaxies.

The star formation rate (SFR) of the *HST* source estimated from the UV continuum and from the Ly- α line and corrected for lensing are $\text{SFR}_{\text{UV}} \sim 5 M_{\odot} \text{ yr}^{-1}$ and $\text{SFR}_{\text{Ly}\alpha} \sim 15 M_{\odot} \text{ yr}^{-1}$. The *Spitzer* detection of 6.3 at $3.6 \mu\text{m}$ implies $(\text{H}-3.6) \approx 2$, redder than for typical $z \sim 6\text{--}8$ LBGs (McLure et al. 2011). SED fits with

² In a recent paper Bradley et al. (2013) mention a quintuple system in this cluster but they list only 3 of our identified images (6.1, 6.3 and 6.4). After the submission of our letter two other articles appeared online (Monna et al. 2013; Balestra et al. 2013) describing in more detail this system and providing a similar spectroscopic redshift. We confirm the fifth image identified by these authors and show it in the Fig. 2 as "6.5".

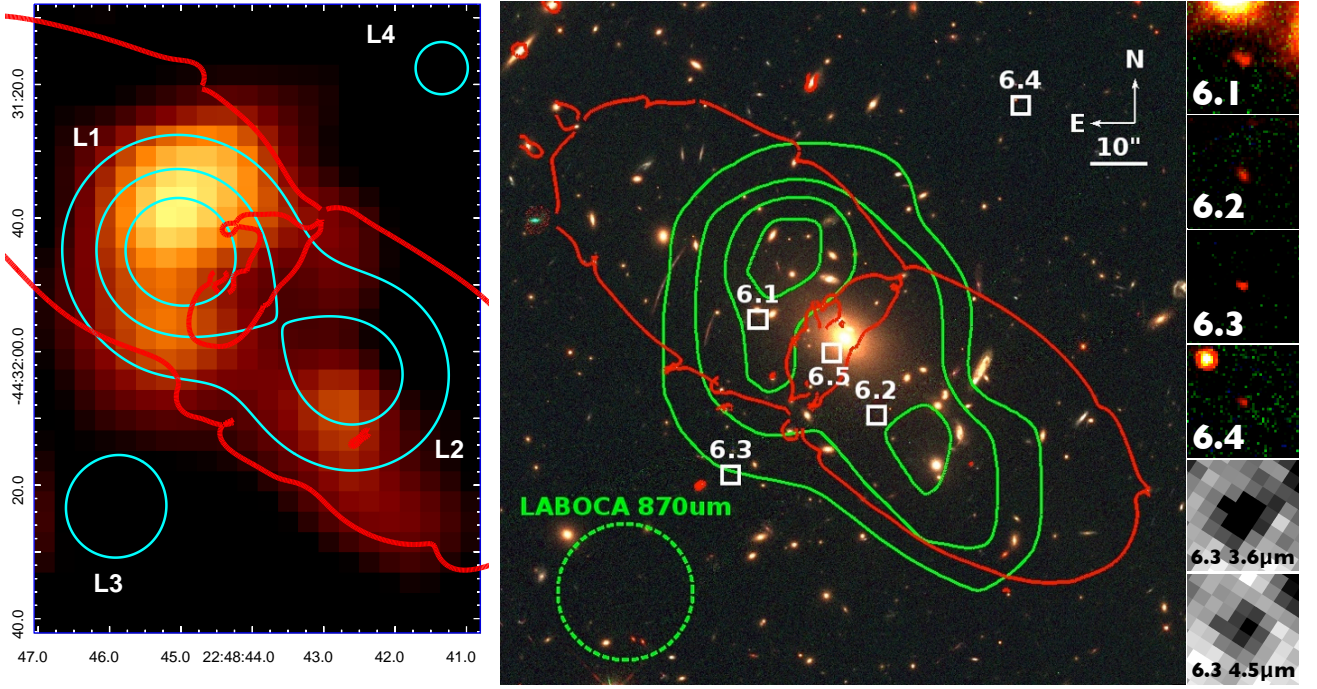


Fig. 2. **Left:** Residuals of the $870\mu\text{m}$ emission after subtraction of the two low- z sources. The cyan contours represent the $z = 6$ source model lensed by the cluster and observed at the resolution of LABOCA. The four images formed are labeled L1, L2, L3 and L4. The contour levels are at 0.25, 0.5 and $0.75 \times S_{L1}$, where S_{L1} is the peak flux of the L1 image. The critical lines for $z = 6$ are overlaid in red. **Right:** *HST* color image of the center of the cluster AS1063 made from images in the filters F606W (blue), F775W (green) and F125W (red). The white squares show the positions of the 4 images of a $z = 6.1$ background source. The thumbnails on the right are $3'' \times 3''$ zooms into these 4 images. The green contours show the $870\mu\text{m}$ emission at 2.6, 3.9, 5.2 and 6.5 mJy (RMS=1.1 mJy). The dotted green circle represents the LABOCA beam (FWHM=24.3'').

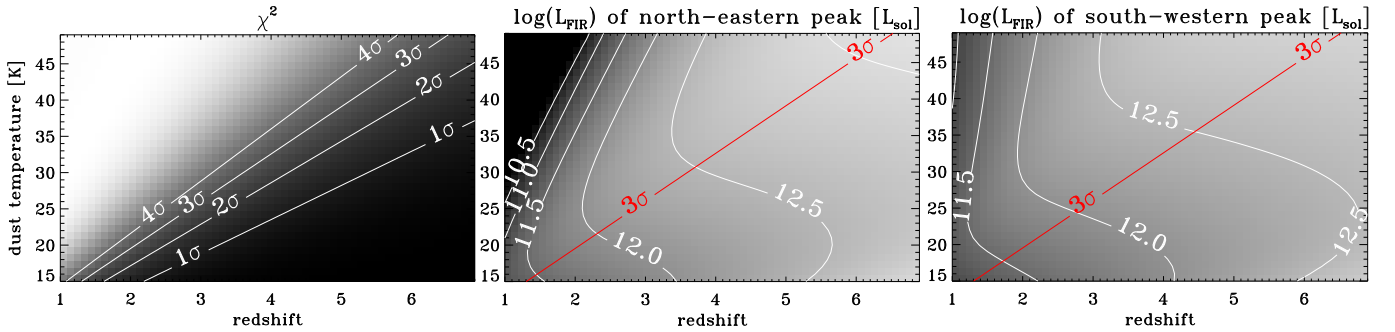


Fig. 3. **Left panel:** χ^2 map in the z - T_d plane, where z and T_d are the redshift and the dust temperature assumed for the $870\mu\text{m}$ source detected with LABOCA. The two $870\mu\text{m}$ -peaks shown in the Fig. 2 as well as the two low- z sources (at $z = 0.6$ and 0.3) shown in the Fig. 1 are fitted simultaneously at all wavelengths from 100 to $870\mu\text{m}$ assuming a modified black body SED for each source (7 free parameters). The white contours show the 1σ , 2σ , 3σ , 4σ confidence levels. **Middle and right panels:** the best fit FIR luminosity in log and without any lensing correction in the z - T_d plane for the two $870\mu\text{m}$ peaks. The white contours are spaced by 0.5 dex. The χ^2 3σ confidence level is over-plotted in red.

young populations predict up to $A_v \sim 1.5$ implying a reprocessed IR luminosity of $\sim 4 \times 10^{11} L_\odot$, i.e., an $\text{SFR}_{\text{IR}} \sim 70 M_\odot \text{yr}^{-1}$.

At $z = 6.1$ the upper limit on the FIR luminosity of the $870\mu\text{m}$ source depends on the SED template assumed as illustrated on the right panel of Fig. 4. The intrinsic luminosities obtained are in the range $[5 - 15] \times 10^{11} L_\odot$, which corresponds to an SFR in the range $[80 - 260] M_\odot \text{yr}^{-1}$. The star forming properties of the *HST* and the LABOCA sources could therefore be similar.

4.4. SZ substructure in the merging cluster?

AS1063 is known to yield a strong SZ effect (Plagge et al. 2010) that was detected at $S/N \sim 17$ with *Planck* (Planck Collaboration et al. 2013). Furthermore, Gómez et al. (2012) showed that this cluster is undergoing a major merging event close to the plane of the sky and there has been growing evidences in recent years, both from observations and simulations, that such a merging configuration can produce small scale substructures in the SZ (Korngut et al. 2011; Mroczkowski et al. 2012; Ruan et al. 2013). These substructures could be caused by shocks and inhomogeneities in the hot gas and their increment could

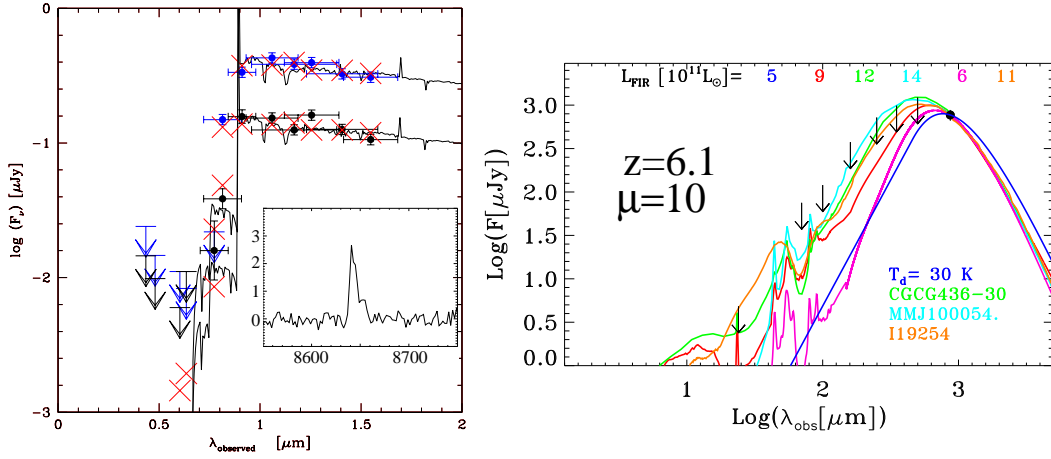


Fig. 4. **Left:** SED fits to the *HST*/ACS-WFC3 photometry of the images B and D (A is contaminated by a nearby source, C is in a noisy strip of the detector). The best fits give $z = 6.3 \pm 0.3$. The inset shows the VLT/FORS spectrum of the B image with the Ly- α line clearly detected at $z = 6.107$ (Richard et al in prep). The x-axis of the inset corresponds to the observed wavelength in Å. **Right:** SED fits to the 870 μ m northern peak taking into account the upper limits listed in the Table 1 and assuming $z = 6.1$ and $\mu = 10$ (all the fluxes are corrected for magnification). The modified black body SED with $T_d = 30$ K is shown in blue, it gives a FIR luminosity $L_{\text{FIR}} = 5 \times 10^{11} L_{\odot}$. The other templates come from the the Chary & Elbaz (2001) library (red), the Vega et al. (2008) library (green), the Michałowski et al. (2010a,b) library (cyan) and the Polletta et al. (2007) library (orange). The template in magenta corresponds to the SMM J2135-0102 model (Swinbank et al. 2010; Ivison et al. 2010).

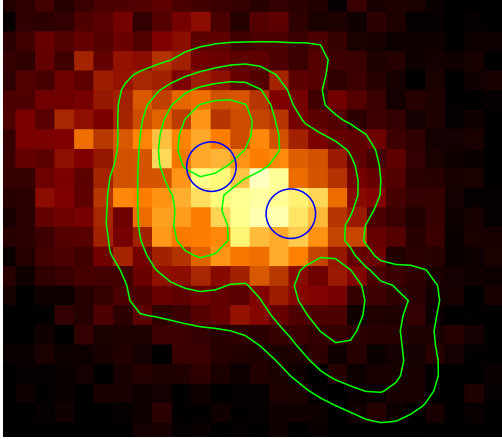


Fig. 5. Chandra X-ray map of AS1063 overlaid with the LABOCA residuals in green contours starting at 2σ and spaced by 1σ . The blue circles mark the positions the two components of the β -model fitted by Gómez et al. (2012) to the Chandra data.

peak at 300-400 GHz (i.e., 750-1000 μ m, Ruan et al. 2013). The SED of such SZ substructures could therefore be consistent with the *Herschel* and LABOCA photometry. Also we note that the northern LABOCA peak is close to the secondary mass component identified by Gómez et al. (2012) (Fig. 5) and its elongated morphology would be consistent with shocked gas. The large scale SZ would be filtered out by the LABOCA observations and the data reduction, and we would be seeing the substructures related to the merging event. More quantitatively, the *Planck* measurement at 353 GHz (the central pixel is at 0.12 MJy/sr) can be used to scale the SZ profile modeled by Plagge et al. (2010) for this cluster and thus estimate the peak flux expected at the center of the LABOCA map ignoring spatial filtering. We obtain ~ 7 mJy/beam. The fraction of this flux filtered by the observations is difficult to estimate from the data because it depends on the morphology of the SZ increment. This will be studied in a forthcoming paper by Zemcov et al. (in prep).

5. Conclusion

With APEX/LABOCA we have detected an extended 870 μ m source aligned with the center of the cluster AS1063. The source is not detected at shorter FIR/submm wavelengths. We find two possible interpretations of this peculiar source, it could be the dusty component of an HST-detected strongly-lensed galaxy at $z=6.1$ or substructures in the SZ effect. The current observations do not allow us to disentangle the two interpretations.

There are two routes to decide between the different origins of the features we have discovered: submm observations with ALMA should allow us to resolve the four images of the high- z source, while lower frequency observations (150 GHz) are required to measure the decrement of the SZ substructures.

Acknowledgements. We are very grateful to the APEX staff for their great help with the observations and their nice welcome at the Sequitor base. We gratefully acknowledge the ESO director for the VLT/FORS program DDT 291.A-5027. We kindly acknowledge Etienne Pointecouteau for providing us with the *Planck* data and for useful discussions. This work received support from the Agence Nationale de la Recherche bearing the reference ANR-09-BLAN-0234. JPK thanks support from the European Research Council (ERC) advanced grant Light on the Dark (LIDA) and CNRS. IRS acknowledges support from STFC (ST/I001573/1), a Leverhulme Fellowship, the ERC Advanced Investigator programme DUSTYGAL 321334 and a Royal Society/Wolfson Merit Award. AMS acknowledges an STFC Advanced Fellowship through grant ST/H005234/1. KK thanks the Swedish Research Council for support (grant 621-2011-5372).

References

- Balestra, I., Vanzella, E., Rosati, P., et al. 2013, arXiv/1309.1593
- Blain, A. W., Barnard, V. E., & Chapman, S. C. 2003, MNRAS, 338, 733
- Blain, A. W., Smail, I., Ivison, R. J., Kneib, J.-P., & Frayer, D. T. 2002, Phys. Rep., 369, 111
- Bradley, L. D., Zitrin, A., Coe, D., et al. 2013, arXiv/1308.1692
- Capak, P. L., Riechers, D., Scoville, N. Z., et al. 2011, Nature, 470, 233
- Chapman, S. C., Blain, A. W., Smail, I., & Ivison, R. J. 2005, ApJ, 622, 772
- Chary, R. & Elbaz, D. 2001, ApJ, 556, 562
- Combes, F., Rex, M., Rawle, T. D., et al. 2012, A&A, 538, L4
- Egami, E., Rex, M., Rawle, T. D., et al. 2010, A&A, 518, L12+
- Gómez, P. L., Valkonen, L. E., Romer, A. K., et al. 2012, AJ, 144, 79
- Hatsukade, B., Ohta, K., Seko, A., Yabe, K., & Akiyama, M. 2013, ApJ, 769, L27

- Iverson, R. J., Swinbank, A. M., Swinyard, B., et al. 2010, *A&A*, 518, L35+
- Karim, A., Swinbank, A. M., Hodge, J. A., et al. 2013, *MNRAS*, 432, 2
- Knudsen, K. K., Kneib, J.-P., Richard, J., Petitpas, G., & Egami, E. 2010, *ApJ*, 709, 210
- Korngut, P. M., Dicker, S. R., Reese, E. D., et al. 2011, *ApJ*, 734, 10
- Magnelli, B., Lutz, D., Santini, P., et al. 2012, *A&A*, 539, A155
- McLure, R. J., Dunlop, J. S., de Ravel, L., et al. 2011, *MNRAS*, 418, 2074
- Michałowski, M., Hjorth, J., & Watson, D. 2010a, *A&A*, 514, A67+
- Michałowski, M. J., Watson, D., & Hjorth, J. 2010b, *ApJ*, 712, 942
- Monna, A., Seitz, S., Greisel, N., et al. 2013, arXiv/1308.6280
- Mroczkowski, T., Dicker, S., Sayers, J., et al. 2012, *ApJ*, 761, 47
- Plagge, T., Benson, B. A., Ade, P. A. R., et al. 2010, *ApJ*, 716, 1118
- Planck Collaboration, Ade, P. A. R., Aghanim, N., et al. 2013, arXiv/1303.5089
- Polletta, M., Tajer, M., Maraschi, L., et al. 2007, *ApJ*, 81
- Rawle, T. D., Chung, S. M., Fadda, D., et al. 2010, *A&A*, 518, L14+
- Rawle, T. D., Edge, A. C., Egami, E., et al. 2012, *ApJ*, 747, 29
- Riechers, D. A., Bradford, C. M., Clements, D. L., et al. 2013, *Nature*, 496, 329
- Ruan, J. J., Quinn, T. R., & Babul, A. 2013, *MNRAS*, 432, 3508
- Siringo, G., Kreysa, E., Kovács, A., et al. 2009, *A&A*, 497, 945
- Smail, I., Iverson, R. J., & Blain, A. W. 1997, *ApJ*, 490, L5
- Swinbank, A. M., Smail, I., Longmore, S., et al. 2010, *Nature*, 464, 733
- Symeonidis, M., Vaccari, M., Berta, S., et al. 2013, *MNRAS*, 431, 2317
- Vega, O., Clemens, M. S., Bressan, A., et al. 2008, *A&A*, 484, 631
- Vieira, J. D., Marrone, D. P., Chapman, S. C., et al. 2013, *Nature*, 495, 344
- Walter, F., Decarli, R., Carilli, C., et al. 2012, *Nature*, 486, 233
- Weiß, A., De Breuck, C., Marrone, D. P., et al. 2013, *ApJ*, 767, 88